



Premiere Publications from The Triological Society

Read all three of our prestigious publications, each offering high-quality content to keep you informed with the latest developments in the field.



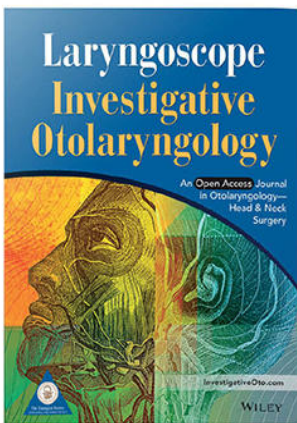
THE Laryngoscope

FOUNDED IN 1896

Editor-in-Chief: Samuel H. Selesnick, MD, FACS

The leading source for information in head and neck disorders.

Laryngoscope.com



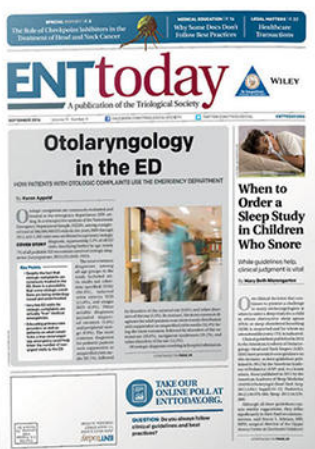
Laryngoscope Investigative Otolaryngology

Open Access

Editor-in-Chief: D. Bradley Welling, MD, PhD, FACS

Rapid dissemination of the science and practice of otolaryngology-head and neck surgery.

InvestigativeOto.com



ENTtoday

A publication of the Triological Society

Editor-in-Chief: Alexander Chiu, MD

Must-have timely information that Otolaryngologists-head and neck surgeons can use in daily practice.

Enttoday.org

WILEY

Antifibrotic Role of Nintedanib in Tracheal Stenosis After a Tracheal Wound

Yuhua Fan, MD; Xin Li, MD; Xing Fang, MD; Yalan Liu, PhD; Suping Zhao, MD; Zicheng Yu, PhD;
 Yaoyun Tang, MD; Ping Wu, MD 

Objectives/Hypothesis: Tracheal stenosis is an obstructive disease of the upper airway that commonly develops as a result of abnormal wound healing. We evaluated the anti-inflammatory and antifibrotic properties of nintedanib on tracheal stenosis both *in vitro* and *in vivo*.

Study Design: Prospective controlled animal study and *in vitro* comparative study of human cells.

Methods: An animal model of tracheal stenosis was induced via tracheal trauma. Postsurgical rats were orally administered with nintedanib (10 or 20 mg/kg/d) or saline (negative control) for 2 weeks, and tracheal specimens were harvested after 3 weeks. Degree of stenosis, collagen deposition, fibrotic surrogate markers expression, and T-lymphocytic infiltration were evaluated. Human fetal lung fibroblast-1 (HFL-1) cells were cultured to determine the effects of nintedanib on changes of cellular biological function induced by transforming growth factor- β 1 (TGF- β 1).

Results: Rat tracheal stenotic tissues exhibited thickened lamina propria with irregular epithelium, characterized by significantly increased collagen deposition and elevated TGF- β 1, collagen I, α -SMA and fibronectin expressions. Nintedanib markedly attenuated the tracheal stenotic lesions, reduced the collagen deposition and the expression of fibrotic marker proteins, and mitigated CD4+ T-lymphocyte infiltration. Additionally, cellular proliferation and migration were decreased dose-dependently in TGF- β 1-stimulated HFL-1 cells when treated with nintedanib. Furthermore, nintedanib inhibited TGF- β 1-induced HFL-1 differentiation and reduced the mRNA levels of the profibrotic genes. TGF- β 1-activated phosphorylation of the TGF- β /Smad2/3 and ERK1/2 pathways were also blocked by nintedanib.

Conclusion: Nintedanib effectively prevented tracheal stenosis in rats by inhibiting fibrosis and inflammation. The antifibrotic effect of nintedanib may be achieved by inhibiting fibroblasts' proliferation, migration and differentiation and suppressing the TGF- β 1/Smad2/3 and ERK1/2 signaling pathways.

Key Words: Tracheal stenosis, nintedanib, fibrosis, fibroblast, TGF- β 1.

Level of Evidence: NA

Laryngoscope, 00:1–10, 2021

INTRODUCTION

Tracheal stenosis (TS) is an uncommon disease caused by repeated injury and repair of the tracheal mucosa and hyperplasia of the resultant granulation tissue.¹ TS is a chronic inflammatory process that can result from several possible etiologies, where the most common being long-term mechanical ventilation with endotracheal intubation. Myriad additional etiologies can also result in luminal compromise of the proximal airway including neck

trauma, tracheotomy, infection (i.e. tuberculosis), and vasculitis (i.e. Wegener's granulomatosis, aka granulomatosis with polyangiitis). Fibroinflammatory airway obstruction can also occur without antecedent injury (i.e. idiopathic subglottic stenosis, iSGS).^{2,3} Ischemia, edema, inflammation, and finally fibrosis, which are caused by compression of the tracheal sleeve, play vital roles in the TS pathogenesis, with an incidence of 0.6% to 21%.⁴

TS formation is a complex and multistage pathophysiological process. When tracheal injuries or infection occurs, platelets, inflammatory cells, epithelial cells, and fibroblasts are attracted to the provisional wound, and angiogenesis and extracellular matrix (ECM) deposition are increased, thus creating a layer that covers the wound surface during the healing process. However, when a wound repairing response goes out of control, many fibroblasts are stimulated by transforming growth factor- β 1 (TGF- β 1) to transform into myofibroblasts, which initiate collagen I and III deposition and wound contraction, resulting in excessive ECM accumulation and fibrotic formation.⁵ TGF- β 1, a key cytokine involved in fibrogenesis, is elevated in many fibrotic processes and exerts its profibrotic effects on fibroblasts by activating the Smad2/3 signaling pathways.⁶ Other chemokines, cytokines, and growth factors, such as platelet-derived

From the Department of Otorhinolaryngology Head and Neck Surgery (Y.F., X.L., X.F., Y.L., S.Z., Y.T., P.W.), Xiangya Hospital of Central South University, Changsha, China; Province Key Laboratory of Otolaryngology Critical Diseases (Y.F., X.L., X.F., Y.L., S.Z., Y.T., P.W.), Xiangya Hospital of Central South University, Changsha, China; and the Cancer Genomics (Z.Y.), GenePlus-Shenzhen, Shenzhen, China.

Additional supporting information may be found in the online version of this article.

Editor's Note: This Manuscript was accepted for publication on April 27, 2021.

Y.F. and X.L. contributed equally to this work.

The authors have no funding, financial relationships, or conflicts of interest to disclose.

Send correspondence to Ping Wu, Xiangya Hospital of Central South University, No. 87 Xiangya Road, Changsha, China. E-mail: wupingcsu@hotmail.com

Yaoyun Tang, Xiangya Hospital of Central South University, No. 87 Xiangya Road, Changsha, China. E-mail: yaoyuntang@outlook.com

DOI: 10.1002/lary.29618

growth factor, fibroblast growth factor (FGF), connective tissue growth factor (CTGF), and vascular endothelial growth factor (VEGF), are also important stimuli in fibrotic processes.⁷ Furthermore, dysregulation of immune cells also gives rise to the pathologic ECM deposition and fibroblast hyperproliferation. Prior work showed increased Th2 cells and M2 macrophages were observed in animal models and patients with iatrogenic LTS (iLTS).^{8–10} Elevated expression of PD-1/PD-L1 axis has also been implicated in the patients with LST.¹¹

Nintedanib is a triple tyrosine kinase inhibitor and growth factor antagonist that targets VEGF receptors, PDGF receptors (PDGFRs), and FGF receptors. The Food and Drug Administration approved nintedanib for treating idiopathic pulmonary fibrosis.¹² Several studies found that nintedanib reduced the TGF-β1-induced phosphorylation of Smad2/3, p38 MAPK, and ERK1/2, showing that nintedanib works through both classic and nonclassic TGF-β1 signaling pathways to inhibit fibroblast activation.¹³ Nintedanib also exhibited consistent antifibrotic and anti-inflammatory activities in animal models of pulmonary fibrosis¹⁴ and interfered with central fibrotic processes such as fibroblast proliferation, migration, differentiation, and ECM protein secretion.¹⁵ Nintedanib exerts significant antifibrotic effects in other organs; therefore, we speculated that it may play similar roles in tracheal fibrosis.

In this study, we aim to translate nintedanib to our preclinical rat model to study its potential role as a medical therapy for TS. We aimed to evaluate the effect of nintedanib on the process of fibrosis and inflammation in TS of rats, as well as on the inhibition of fibrogenesis in fibroblasts, attempting to offer a novel therapeutic approach for treating TS.

MATERIALS AND METHODS

Experimental Animals and Ethics Statement

Experimental Sprague-Dawley (SD) rats were provided by the Zoology Department of Central South University. The rats were housed in a temperature- and humidity-controlled room on a 12-hour light/dark cycle and given free access to water and food. All experimental procedures followed the International Guiding Principles for Biomedical Research Involving Animals issued by the Council for the International Organizations of Medical Sciences and were approved by the Ethics Committee of Xiangya Hospital of Central South University. Eight-week-old male SD rats weighing 250 to 350 g were used.

Animal Model of Tracheal Scar Stenosis

Generally, surgical technique used in this study followed the method established by Hillel et al. in murine LTS.¹⁶ However, to avoid the antagonistic effects on nintedanib, we did not use bleomycin in surgical operation. Briefly, SD rats were anesthetized preoperatively by intraperitoneally administering 300 mg/kg chloral hydrate. The rats could breathe spontaneously throughout the procedure. Anesthetized rats were placed in the supine position. The anterior necks of the rats were shaved, sanitized with 70% ethanol, and covered with sterile towels. A midline vertical skin incision was extended from the upper border of the thyroid cartilage of the incisura jugularis to perform the tracheostomy. Passing through the skin and subcutaneous tissue,

strap muscles were retracted to expose the laryngotracheal framework. A parallel tracheotomy was performed between the third and fourth cervical tracheal rings after separating the anterior tracheal fascia. The tracheal mucosa above the incision was scraped five times with a micro curette to induce artificial tracheal trauma. The tracheas were then stitched carefully using a contraposition suture, and the strap muscles, subcutaneous tissue, and skin were closed anatomically. All rats underwent orotracheal intubation with a 2-mm silicone tube in case of tracheal hemorrhaging or asphyxia. The tube was removed after the rats had completely recovered from the anesthesia.

Grouping and Administration Methods

The rats were observed and followed for any respiratory obstruction during the first 3 postoperative days, and three rats died during the perioperative period. Finally, 30 survived rats were randomized into three groups of 10 rats each. Group I had tracheal trauma and was orally administered with 10 mg/kg/d nintedanib (Selleckchem, Houston, TX) for 14 days. Group II had tracheal trauma and was orally administered with 20 mg/kg/d nintedanib for 14 days. Group III had tracheal trauma and was orally administered with saline solution for 14 days as a negative control. Ten normal rats that did not undergo a tracheotomy or treatment were treated as the normal control group. The animals were sacrificed at 21 days postoperatively by an overdose of 10% chloral hydrate.

Morphometric Evaluation

The rat tracheas were resected between the inferior border of the cricoid cartilage and upper border of the sternum, and the upper sections showing tracheal anastomosis were collected. Each tracheal specimen was fixed in 4% paraformaldehyde, embedded in paraffin, and then inserted in a paraffin block. The embedded samples were cut into 5-μm-thick sections using a Leica RM2235 microtome (Leica Microsystems, Wetzlar, Germany), stained with hematoxylin and eosin (H&E) and Masson's trichrome (MT), and examined using an ECLIPSE Ci microscope (Nikon, Tokyo, Japan). H&E-stained sections were used to measure the tracheal fibrotic thickness using the ruler tool in ImageJ

TABLE I.
Primers of Profibrotic Genes for Real-Time Quantitative Polymerase Chain Reaction Validation.

Symbol	Primer sequence 5'-3'
FGF2	F: CAAGCAGAAGAGAGAGAGTTG R: CGTAACACATTAGAACGCCAGTAATC
FGF7	F: CTTGAGGTCAAGCCTACAGATAAC R: ACCTCCCATTGGTGAACATATAA
CTGF	F: CATTCTCCAGCCATCAAAGAGAC R: CCACAAGCTGTCCAGCTAAATC
VEGF	F: GAGCTTCTACAGCACAAACA R: CCAGGACTTACCGGGATTTC
TGFB1	F: TTCAGTCACCATAGCAACACTC R: GAACTCCTCCCTAACCTCTCT
PDGF	F: GGACAGTGCAGCGGTATTT R: GGAGAAACACAAAGCCAGAAC
GAPDH	F: CAGGGCTGCTTTAACCTCTGG R: TGGGTGGAATCATATTGGAACA

graphic software. MT-stained sections were evaluated for tracheal collagen deposition using the ImageJ graphic analysis system.

Immunohistochemical and Immunofluorescent Evaluation

Additional 5- μ m-thick sections were created for immunohistochemical (IHC) examination. Sections were stained by processing with anti-TGF- β 1 antibody (AF1027, Affinity, Wuhan, China), anti-alpha smooth muscle actin antibody (α -SMA; A17910, Abclonal, Wuhan, China), anti-collagen I antibody (A16699, Abclonal, Wuhan, China), and fibronectin antibody (ab2413, Abcam, Cambridge, UK) using an enhanced polymer detection system kit (pv-9001/2, Beijing Zhongshan

Jinqiao Biotechnology, Beijing, China). The sections were incubated with 3,3'-diaminobenzidine tetrahydrochloride (DAB, Beijing Zhongshan Jinqiao Biotechnology) and counterstained with hematoxylin (Beijing Zhongshan Jinqiao Biotechnology). Protein expression scores were quantified by measuring the average optical density using ImageJ graphics analysis, which was based on the degree of brown staining for the entire sample. Eight to 10 sections from each animal were blindly analyzed by the observers.

For immunofluorescent multiplex staining, tyramide signal amplification was performed according to the Opal 4-Color Manual IHC Kit (Perkin Elmer, Waltham, MA). Sections were sequentially stained with primary antibodies (anti-rat CD3 and CD4, anti-rat CD3 and CD8) and horseradish peroxidase-labeled secondary antibody, followed by incubation with detection reagents Opal 520 (green), Opal 570 (red), and Opal DAPI (blue).

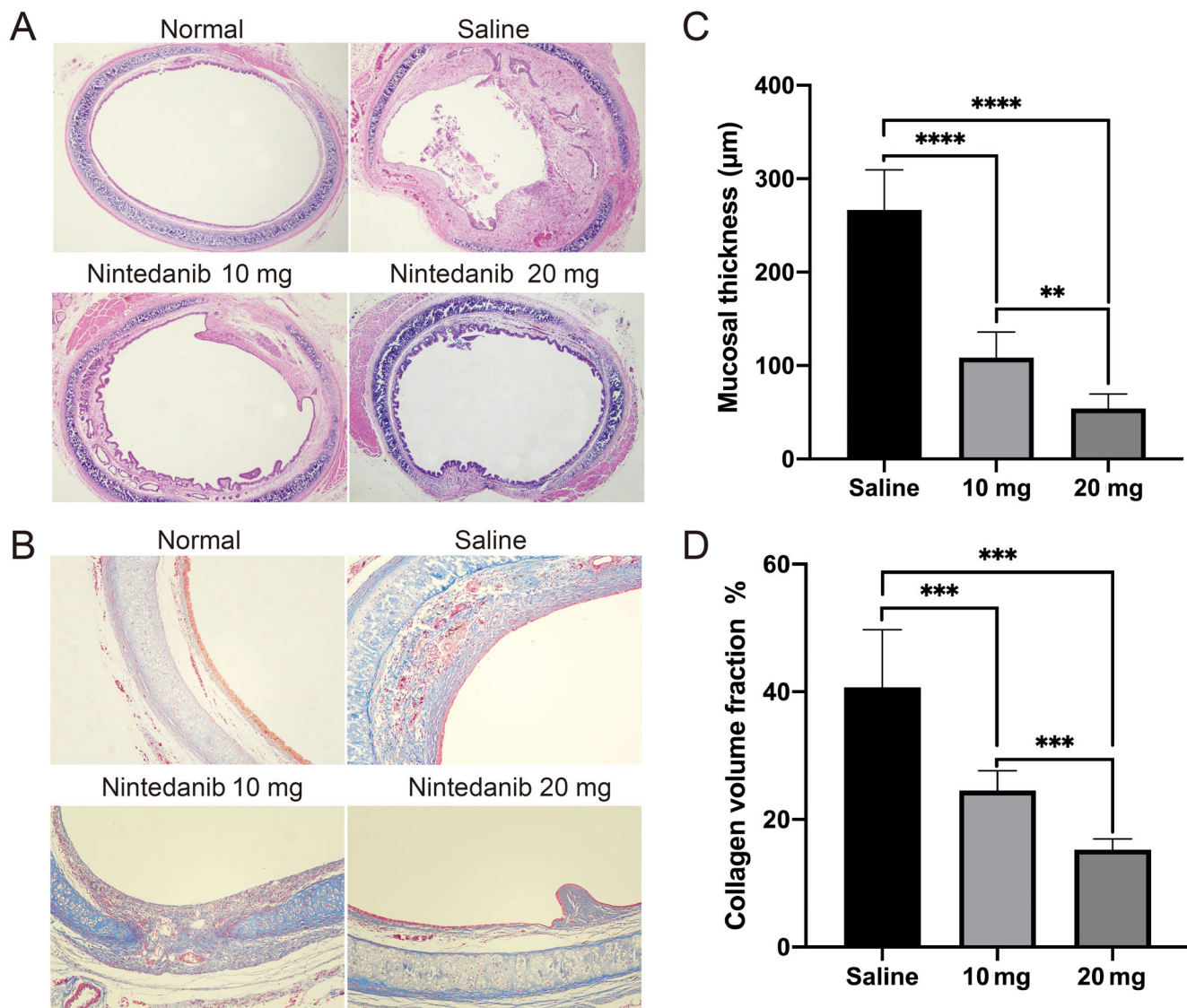


Fig. 1. Histopathological evaluation of tracheal stenosis model in rats. (A) Representative images of hematoxylin and eosin staining tracheal tissue section from saline and nintedanib (10 mg, 20 mg) treated groups, rats without any treatment as normal control ($\times 50$). (B) Representative images of Masson's trichrome staining tracheal tissue section from control, saline, and nintedanib (10 mg, 20 mg) treated groups ($\times 200$). (C) Quantification of tracheal thickening in saline and nintedanib (10 mg, 20 mg) treated groups. (D) Quantification of collagen volume fraction in saline and nintedanib (10 mg, 20 mg) treated groups. Data shown are means \pm standard error of mean (SEM). ** P < .01, *** P < .001, **** P < .0001; ns = not significant. [Color figure can be viewed in the online issue, which is available at www.laryngoscope.com.]

The slides were imaged using a laser scanning confocal microscope (Leica TCS SP8, Germany) and LAS X software (Leica, Microsystems, Germany). Quantification of lymphocytes was performed by counting the positive-stained cells at high magnification ($\times 400$) from three areas with intense inflammation determined at low magnification ($\times 100$).⁹ The percentage of lymphocytes was calculated by dividing the number of positive cells by the total number of cells in the high-power field. The detailed information of employed antibodies is shown in Table S1.

Cell Culturing

Human fetal lung fibroblast-1 (HFL-1) cells were purchased from Procell (Wuhan, China) and cultured in Dulbecco's modified Eagle's medium (DMEM; BI, Israel) containing 8% fetal bovine serum (FBS; BI) and 1% penicillin-streptomycin (NCM Biotech, Suzhou, China). Cells were grown at 37°C under 5% CO₂ in a humidified atmosphere.

Cell Viability Assays

HFL-1 cells were plated in 96-well plates (3,000 cells/well) in 100 µl DMEM and divided into five groups: (i) control: cells were incubated with dimethyl sulfoxide (DMSO) (1 µm); (ii) TGF-β1 (R&D Systems, Minneapolis, MN), cells were incubated with TGF-β1 (5 ng/ml) and DMSO (1 µm); (iii) cells were treated with TGF-β1 (5 ng/ml) and 1 or 2 µM of nintedanib, respectively. The drugs and cells were incubated for 24, 48, and 72 hours. DMSO, which was used to dissolve the nintedanib, was added to the control and TGF-β1 groups. Next, 10 µl of cell-counting CCK-8 kit

(NCM Biotech, Suzhou, China) solution was added to each well and incubated for 1 hour at 37°C. The absorbance was measured at 450 nm using an enzyme-labeling instrument (BioTek, Winooski, VT).

Wound-Healing Assays

Cells were seeded in six-well plates and grown to confluence. The cells were starved overnight by removing the serum, and a vertical wound was created using a 200-µl pipette tip. The cells were then washed three times with phosphate-buffered saline (PBS) and replaced with fresh DMEM containing 0.2% FBS and 1 or 2 µM of nintedanib. After 24 or 48 hours, the cells were washed three times with PBS, and the scratched distance was detected with ImageJ.

Transwell Invasion Assay

The cell migration ability was measured using the Boyden blind-well chamber technique (Costar, New York, NY). The four cell groups were the same as those in the wound-healing assays. Briefly, 18,000 cells suspended in FBS-free DMEM with 1 or 2 µM nintedanib were transferred to the upper chamber, with DMEM containing 8% FBS placed in the lower chamber. The two wells of the Boyden blind-well chamber were separated by an 8-µM pore filter (Corning, Bedford, MA). After 48 hours of incubation at 37°C, noninvasive cells were scraped, and migrated cells were fixed in methanol and stained with 0.2% crystal violet. ImageJ software was used to count the cells.

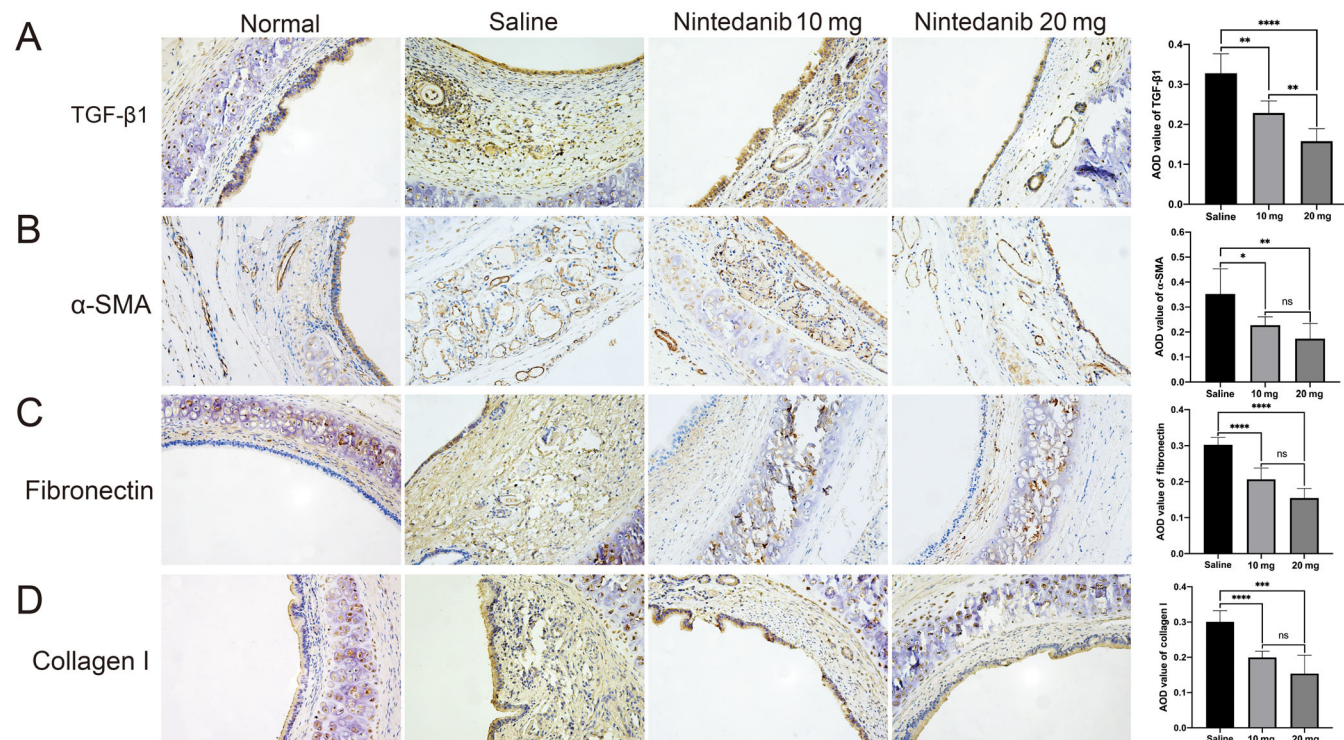


Fig. 2. Immunohistochemical detection of transforming growth factor-β1 (TGF-β1), α-SMA, fibronectin, and collagen I expression in tracheal scar tissues from normal, saline, and nintedanib (10 mg, 20 mg) treated rat groups. (A) TGF-β1 was detected in both the epithelial and submucosal layers ($\times 200$); (B) α-SMA was detected in fibroblasts in submucosal layers ($\times 200$); (C,D) fibronectin and collagen I were expressed in the intercellular substance and submucosal cells in the stenotic tissues ($\times 200$). Average optical density (AOD) date of four antibodies are presented as the means \pm SEM. * $P < .05$, ** $P < .01$, *** $P < .001$, **** $P < .0001$ compared with saline-treated group; ns = not significant. [Color figure can be viewed in the online issue, which is available at www.laryngoscope.com.]

Real-Time Quantitative Polymerase Chain Reaction

Real-time quantitative polymerase chain reaction (RT-qPCR) analysis was performed on a QuantStudio7 Flex (Life Technologies, Carlsbad, CA). Total RNA was extracted with TRIzol reagent (Life Technologies, Shanghai, China), and 1 µg was retrotranscribed using the First-Strand cDNA Synthesis Kit (Genecopeia, Guangzhou, China). Reverse-transcribed cDNAs were amplified in duplicate using the All-in-One™ mRNA detection kit (Genecopeia, Guangzhou, China) based on SYBR-Green Life Technologies designed and synthesized the primers. The PCR reaction was carried out under the following thermocycling conditions: 95°C for 30 seconds, then 40 cycles of 95°C for 10 seconds, and 60°C for 30 seconds. Relative mRNA expression was normalized using the GAPDH gene. Each sample was run in triplicate and repeated in three independent experiments. The primer sequences are listed in Table I.

Western Blot

The experimental steps followed our previous approaches.¹⁷ Briefly, protein was extracted with RIPA lysis

buffer, and the concentration was detected by BCA Protein assay kit (Thermo Scientific, Waltham, MA). Proteins were separated using 10% SDS-PAGE and transferred to PVDF membranes, then the membranes were incubated with primary antibodies and appropriate secondary antibodies successively. The bands were detected using a Bio-Rad (Hercules, CA) imaging system. All the detailed information of the employed antibodies is provided in Table S1.

Statistical Analysis

GraphPad Prism v8.00 for Windows (GraphPad Software, San Diego, CA) was used for the statistical analyses. Normality was tested with the Shapiro-Wilk normality test. For the normally distributed countable data, independent-sample *t*-tests were used for between-group comparisons. Percentages of lymphocytes from different groups were compared using a Fisher's exact test. Multiple groups were compared via analysis of variance. The Bonferroni test was used for post-hoc pairwise comparisons. Differences were considered statistically significant at $P < .05$.

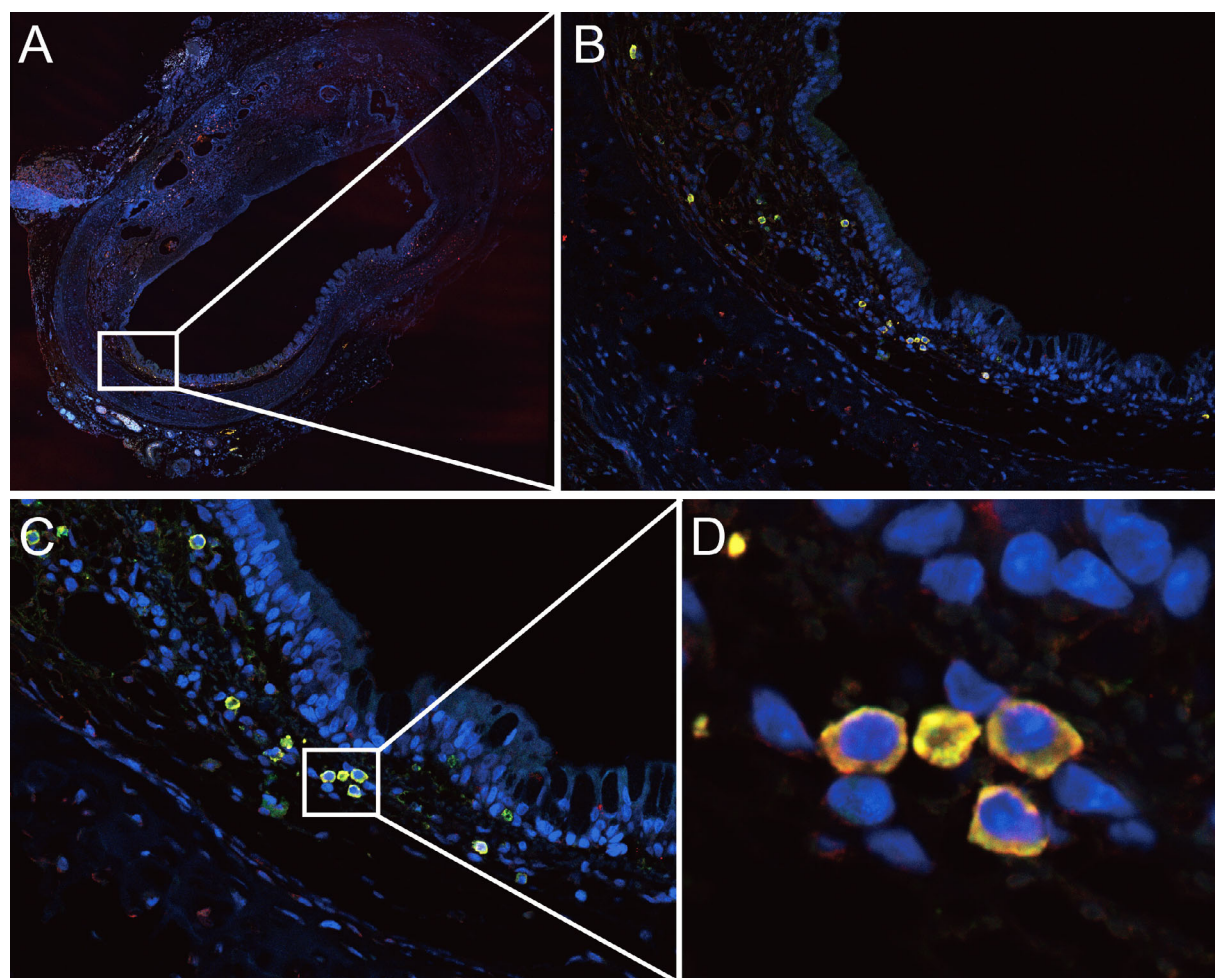


Fig. 3. CD4+ T-cells infiltration in the injured rat trachea detected by immunofluorescence. (A) A representative of photomicrographs was taken of rat thickened lamina propria with CD3+/CD4+ T-cells infiltration ($\times 50$ magnification). (B) Inset, $\times 200$ magnification. (C) Inset, $\times 400$ magnification. (D) A locally magnified picture of the area of CD3+/CD4+ T-cells expression. CD3: green; CD4: red; DAPI: blue. [Color figure can be viewed in the online issue, which is available at www.laryngoscope.com.]

RESULTS

Nintedanib Attenuated Tracheal Fibrosis in Rats' TS Model

To evaluate the potential therapeutic effect of nintedanib on submucosal fibrotic development, rats were treated with either 10 or 20 mg/kg/d nintedanib or a saline vehicle control. Twenty-eight of 30 rats were analyzed at 3 weeks. Two rats in the control group died from respiratory obstruction; no rats died in treatment groups. To analyze the histopathological changes and fibrosis in the rat tracheal tissue, we measured the maximal thickness of the submucosal fibrosis and collagen-stained areas, which were evaluated via H&E and MT staining (Fig. 1A,B). In the saline-treated group, H&E examination revealed TS that was histologically characterized by a conspicuous submucosal fibrotic response, with intense inflammatory cell infiltration. MT staining revealed epithelial hyperplasia and significant submucosal tissue thickening, mainly deposited by collagen, in the fibrotic lesion. Nintedanib treatment markedly reduced the fibrotic lesion and collagen deposition. The thickened submucosal depth and collagen volume

fraction (CVF) were significantly decreased in both nintedanib-treated groups compared with that of the saline-treated group, with the higher-dose group showing stronger fibrotic inhibition (Fig. 1C,D).

Nintedanib Reduced TGF- β 1, Collagen I, α -SMA and Fibronectin Expression, and CD4+ T-Lymphocytic Infiltration in Rats' TS Model

TGF- β 1, which activates the TGF- β profibrotic signaling pathway, is the primary mediator in fibrosis. To assess the effect of nintedanib on the TGF- β signaling cascade, we detected the expressions of TGF- β 1 and several surrogate markers (collagen I, α -SMA, and fibronectin) for TGF- β activation and response via IHC analysis. TGF- β 1 and the three markers were rare in the normal tracheas, whereas TGF- β 1 and α -SMA were significantly increased in both the tracheal epithelial and submucosal cells, and fibronectin and collagen I were overexpressed in the intercellular substance and submucosal cells in the stenotic tissues of saline-treated group. IHC revealed that administering nintedanib markedly reduced tracheal

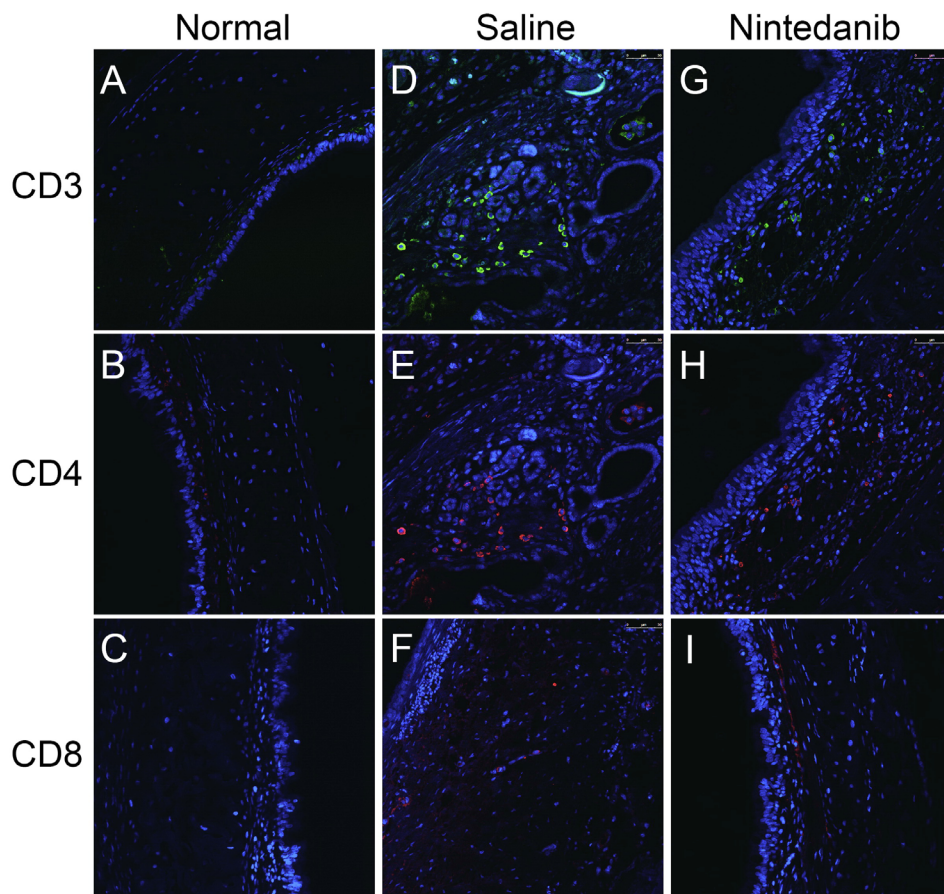


Fig. 4. An immunofluorescence analysis showing the infiltration of T-cells in tracheal tissues. Micrographs showing that no CD3+, CD4+, or CD8+ T-cell infiltration in the normal tracheal mucosa (A, B, C); more intense staining T-cells (D) (CD3: green) or helper T-cells (E) (CD4: red) are seen in the saline-treated tracheal scar tissues, and relatively less in the nintedanib-treated (G, H) group. No CD8+ T-cells (red) were seen in saline-treated (F) or nintedanib-treated (I) specimens. All pictures have been taken at $\times 400$ magnification. [Color figure can be viewed in the online issue, which is available at www.laryngoscope.com.]

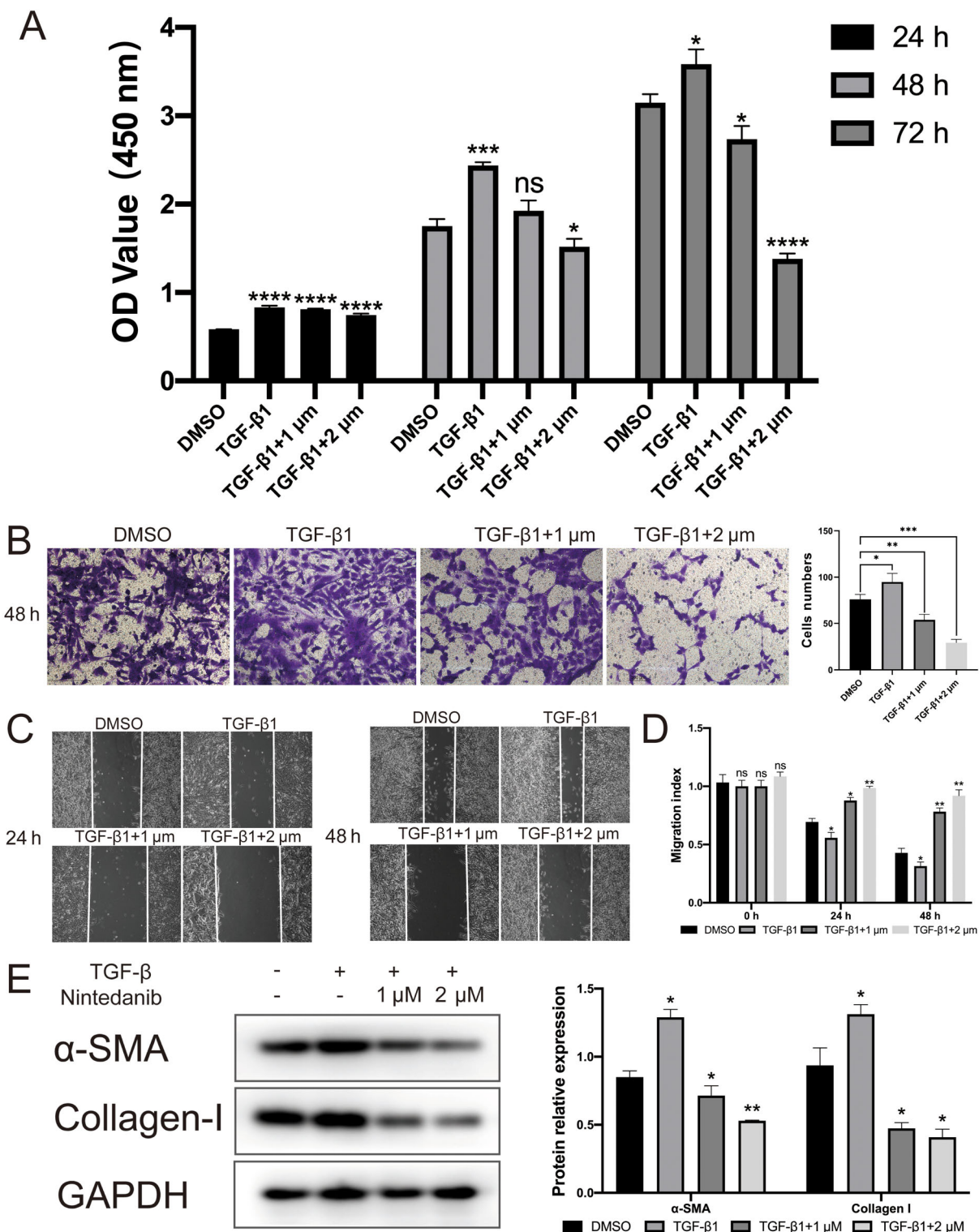


Fig. 5. Effects of nintedanib on transforming growth factor- β 1 (TGF- β 1)-stimulated proliferation, migration, and differentiation in human fetal lung fibroblast-1 (HFL-1) cells. (A) HFL-1 cells were incubated with TGF- β 1 (5 ng/ml) in the presence or absence of nintedanib (1 μ M and 2 μ M) incubation for 24, 48, and 72 hours, cells treated with dimethyl sulfoxide (DMSO) as control. Viability was measured with the CCK-8 reagent. (B) HFL-1 cells migration was determined by transwell assay. Cells were cultured with TGF- β 1 (5 ng/ml) in the presence or absence of nintedanib incubation (1 μ M and 2 μ M) for 48 hours. (C, D) HFL-1 cells healing ability was evaluated by wound healing assay. Cells were treated by TGF- β 1 (5 ng/ml) in the presence or absence of nintedanib (1 μ M and 2 μ M) incubation for 24 and 48 hours. (E) Western blot analysis to analyze the effects of nintedanib on TGF- β 1-mediated targets (α -SMA and collagen I) related to cellular differentiation. HFL-1 cells were cultured in TGF- β 1 (5 ng/ml) in the presence or absence of nintedanib (1 μ M and 2 μ M) incubation for 24 hours. Values represent means \pm SEMs of three separate experiments. * $P < .05$, ** $P < .01$, *** $P < .001$; ns = not significant. [Color figure can be viewed in the online issue, which is available at www.laryngoscope.com.]

trauma-induced TGF- β 1 (Fig. 2A), α -SMA (Fig. 2B), fibronectin (Fig. 2C), and collagen I (Fig. 2D) protein overexpression in both treated groups compared with that in the saline-treated group, part of which presented dose-dependent inhibition.

Multispectral staining of a TS resection specimen demonstrated infiltration of CD3+/CD4+ T-helper cells in the superficial lamina propria (Fig. 3A–D). Staining for additional immune cell markers demonstrated that normal tracheas contained no T-lymphocyte (CD3) or T-helper cell (CD4) or cytotoxic T-lymphocytes (CD8, Fig 4A–C). Compared to saline-treated group, nintedanib (Group II) treated TS rats showed a lower density of CD3+ cell (6.5% vs. 27.4%, $P = .0002$), CD4+ cell (5.1% vs. 15.7%, $P = .0119$), and CD3+/CD4+ cell (4.8% vs. 13.7%, $P = .03$); CD8+ cell was not significantly different between the saline-treated and nintedanib-treated groups (2.6% vs. 3.4%, $P = .3124$, Fig. 4D–I).

Nintedanib Inhibited TGF- β 1-Induced Cell Proliferation and Migration Ability

We used a CCK-8 assay to investigate the effect of nintedanib on the proliferation of HFL-1 cells stimulated with TGF- β 1 alone or with 1 or 2 μ M nintedanib. TGF- β 1 stimulation triggered a significant increase in cell proliferation compared with that of the control cells in different time points (Fig. 5A). Cells co-incubated with TGF- β 1 showed significantly reduced proliferation when treated with nintedanib and the decrease was dose-dependent, in which both 1 and 2 μ M nintedanib notably suppressed the TGF- β 1-induced cell proliferation (Fig. 5A).

Transwell migration assays were used to assess the effect of nintedanib on cell migration. Treating cells with TGF- β 1 for 48 hours increased HFL-1 cell invasion through collagen-coated inserts compared with that of the control cells. Conversely, nintedanib concentration-dependently reduced the TGF- β 1-induced cell penetration (Fig. 5B). We

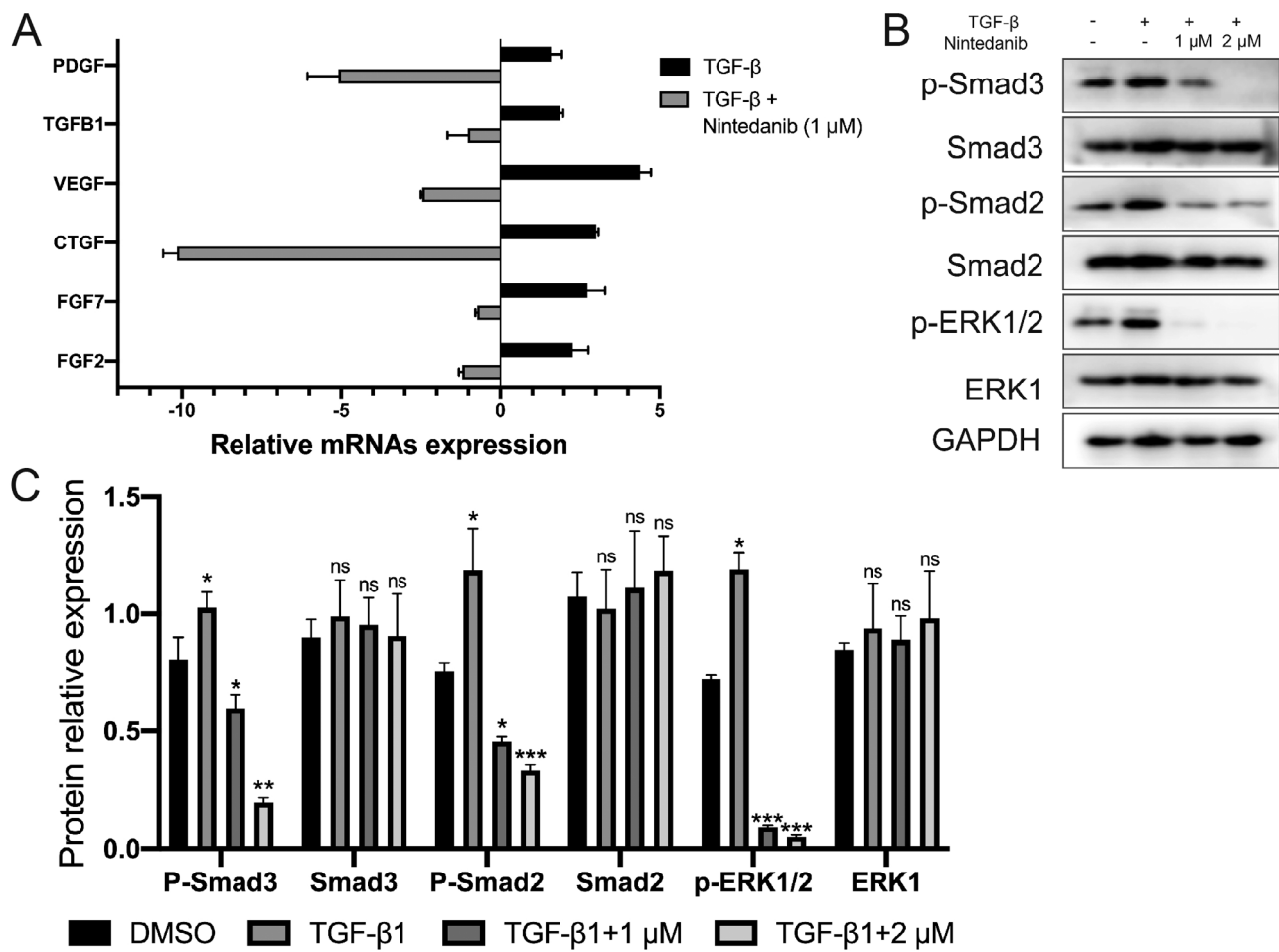


Fig. 6. Effect of nintedanib on transforming growth factor- β 1 (TGF- β 1)-stimulated profibrotic genes expression along with Smad2/3 and ERK1/2 signaling pathway activation. (A) Genes' relative expression was analyzed by real-time quantitative polymerase chain reaction. Data show the fold changes of six different genes in human fetal lung fibroblast-1 cells incubated with TGF- β 1 (5 ng/ml) in the presence or absence of nintedanib (1 μ M) for 24 hours, dimethyl sulfoxide (DMSO)-treated cells as control. (B) Smad2, Smad3, ERK1, and their phosphorylation statuses were determined by western blot. Cells were treated with TGF- β 1 (5 ng/ml) in the presence or absence of nintedanib (1 μ M and 2 μ M) for 6 hours, and expression of GAPDH was used to normalize sample loading. (C) The bar represents the average results (means \pm SEM) from three different experiments.* $P < .05$, ** $P < .01$, *** $P < .001$, **** $P < .0001$; ns = not significant.

next evaluated the effects of nintedanib on cell-healing abilities via two-dimensional wounding assays. Compared with the control cells, TGF- β 1-treated HFL-1 cells enhanced the maximum impedance recovery for 24 and 48 hours. These effects were attenuated by the combination of nintedanib, which dose-dependently reduced the recovery rate (Fig. 5C,D).

Nintedanib Prevented Fibroblasts From TGF- β 1-Induced Differentiation Into Myofibroblasts

Myofibroblasts are characterized by α -SMA expression and are involved in wound contraction, which produces more ECM components than do normal fibroblasts.¹⁸ TGF- β 1 is a strong promotor of fibroblast differentiation into myofibroblasts.¹⁹ To determine whether nintedanib could inhibit TGF- β 1-induced fibroblast differentiation, we treated HFL-1 cells with 5 ng/ml TGF- β 1 in the presence or absence of 1 or 2 μ M nintedanib. Western blot analysis showed that TGF- β 1 treatment significantly elevated α -SMA and collagen I levels after 48 hours compared with that of the vehicle control group. Both 1 and 2 μ M nintedanib reversed this tendency, indicating that coincubation with nintedanib substantially alleviated differentiation and counteracted the effects of TGF- β 1 (Fig. 5E).

Nintedanib Inhibited Profibrotic Gene Expression

To address whether nintedanib affects cytokine and chemokine expression, we used qRT-PCR to detect the RNA expression profiles of eight profibrotic genes (*TGFB1*, *PDGF*, *FGF2*, *FGF7*, *CTGF*, *VEGF*) with nintedanib alone or in the presence of TGF- β 1. TGF- β 1 significantly increased *FGF2*, *CTGF*, and *VEGF* expressions (>2.0-fold) compared with that of the negative controls (Fig. 6A). Conversely, treatment with nintedanib for 24 hours prominently repressed the expressions of these genes in HFL-1 cells. All the gene expressions of nintedanib-treated cells were downregulated by comparison with the control cells (Fig. 6A). Notably, *PDGF* and *CTGF* responded more strongly to nintedanib with a >5.0-fold reduction.

Nintedanib Decreased the TGF- β 1-Stimulated Smad2/3 and ERK1/2 Phosphorylation

TGF- β 1 acts as a profibrotic stimulus by activating the Smad2/3 and p38 MAPK signaling pathways. To reveal the potential molecular targets underlying the inhibitory effects of nintedanib in fibroblasts, we detected the phosphorylation levels of several kinases via western blot. Treatment with 5 ng/ml TGF- β 1 alone significantly increased Smad2/3 and ERK1/2 phosphorylation (Fig. 6B, C). Coincubation with nintedanib markedly suppressed these effects (Fig. 6B,C). These results suggested that nintedanib prevented HFL-1 cell activation by inhibiting the Smad2/3 and ERK1/2 signaling pathways.

DISCUSSION

The main causes of TS are tracheotomies and endotracheal intubation, and their direct injury and possible secondary infections can damage the tracheal wall structure, especially the tracheal mucosa. The main treatments for TS include surgical resection of the narrow tracheal segment, end-to-end anastomosis, T-tube implantation, and endoscopic interventional therapy. Although surgery is the preferred treatment for TS, many patients must undergo multiple surgeries to permanently reduce TS and laryngeal stenosis with decannulation rates of 63% to 89%.²⁰ Consequently, fibrotic development should be prevented before stenosis forms.

Drug therapy is another alternative strategy. Mitomycin C and glucocorticoids, which have anti-inflammatory properties and partial antstenotic effects, are the most common treatments for TS.²¹ Nevertheless, adverse effects and short-term and finite therapeutic efficacy limit the clinical applications of these drugs. Thus, novel drugs with antifibrotic and anti-inflammatory effects that can improve TS treatment efficacy are urgently needed.

Here, we first assessed the role of nintedanib on tracheal wound healing in rats by performing tracheotomies and inducing tracheal trauma to induce stenosis. In the control group, after the surgical procedure, the rats' tracheal tissues showed marked submucosal fibrosis, collagen deposition, and severe histological inflammation accompanied by increased TGF- β 1, collagen I and fibronectin expressions, and α -SMA myofibroblasts. Conversely, rats treated with nintedanib developed mild-to-moderate, dose-dependent, thickened tracheal fibrosis and inflammation. Moreover, the CVF decreased sharply in the drug-treated groups, and the TGF- β 1, collagen I, fibronectin, and α -SMA expressions were attenuated. This study also demonstrated an intense CD3+ and CD4+ T-lymphocytic infiltration in rats' TS specimen, while nintedanib markedly reduced the infiltration of CD3+ and CD4+ lymphocytes. This result presented here is in line with recent publications investigating immune cell presence in murine and human iLTS.^{9,22} Therefore, this animal model provides valid preclinical evidence for developing potential antifibrotic drugs, suggesting that nintedanib exhibits antifibrotic and anti-inflammatory properties over short periods of administration.

We next showed that nintedanib dose-dependently reduced TGF- β 1-stimulated cell proliferation, invasion, and migration in HFL-1 cells. Attenuated cell growth and migration can affect cell infiltration into a wound bed, which may ultimately contribute to stenosis remodeling. We further demonstrated that nintedanib inhibited collagen I and α -SMA (a biomarker of myofibroblasts) expressions in HFL-1 cells. In addition to downregulating these protein expressions in rat fibrotic tissues, nintedanib delayed and inhibited TGF- β 1-induced myofibroblast differentiation. qRT-PCR array results also showed significant changes to fibrosis-related genes. In our in vitro model, nintedanib inhibited the effect of TGF- β 1 by markedly restraining *CTGF* and *PDGF* expression. CTGF is a central mediator of tissue remodeling and fibrosis by stimulating collagen production and enhancing the TGF- β signaling pathway.²³ Nintedanib also downregulated *PDGF*, *TGFB1*,

FGF2, and *FGF7*. Thus, nintedanib exhibits antifibrotic and anti-inflammatory features by inhibiting multiple profibrotic cytokines and growth factors.

TGF- β signaling is activated through canonical Smad2/3 regulation and noncanonical SMAD-independent signaling cascades. TGF- β 1 can also stimulate activation of MAPK signaling cascades, such as p38MAPK and ERK1/2.^{24,25} Additionally, the p38MAPK and ERK1/2 protein kinases have been shown to be involved in PDGF and FGF signaling pathway activation.^{26,27} Because multiple coordinated mechanisms modulate the profibrotic actions of fibroblasts, we investigated how drugs affect the activation of various kinases. Our data showed that SMAD2/3 was upregulated in response to TGF- β 1 stimulation, while nintedanib inhibited TGF- β receptor-activated SMAD2/3 phosphorylation at both concentrations. This is consistent with the previous findings that nintedanib inhibits TGF- β 1-mediated SMAD phosphorylation.²⁸ Furthermore, TGF- β 1 triggered ERK1/2 phosphorylation, and nintedanib treatment repressed ERK1/2 phosphorylation in HFL-1 cells. Based on our findings and previous research,²⁹ interrelated signaling between TGF- β 1/SMAD and PDGFR/ERK1/2 may regulate fibroblast functions during fibrosis.

Our study has certain limitations. Primarily, the use of rat models may not completely reflect the human experience. In human LTS, a significant component of TS was weakened/disordered cartilage ring superstructure as a component of the pathogenic fibrosis. This model treats animals right after isolated mucosal injury, and it remains unclear how nintedanib would impact the clinical course of mature stenosis in humans. Furthermore, HLF-1 cells derived from human lung fibroblast, which possesses different anatomic location and clinical courses from TS, while the use of the HLF-1 cells may not be representative of the cellular subsets to investigate the impact of nintedanib on human TS pathologic fibroblasts.

CONCLUSION

In summary, nintedanib prevented TS by decreasing fibrosis and inflammation in an experimental rat model and alleviated the profibrotic actions of TGF- β 1-stimulated fibroblasts. These results strongly suggest that nintedanib may be a promising antifibrotic agent for laryngotracheal fibrosis prophylaxis and treatment.

BIBLIOGRAPHY

- Huang Z, Wei P, Gan L, Zeng T, Qin C, Liu G. Role of erythromycin-regulated histone deacetylase-2 in benign tracheal stenosis. *Can Respir J* 2020;2020:4213807.
- Gadkaree SK, Pandian V, Best S, et al. Laryngotracheal stenosis: risk factors for tracheostomy dependence and dilation interval. *Otolaryngol Head Neck Surg* 2017;156:321–328.
- Gelbard A, Francis DO, Sandulache VC, Simmons JC, Donovan DT, Ongkasuwan J. Causes and consequences of adult laryngotracheal stenosis. *Laryngoscope* 2015;125:1137–1143.
- Deshmukh A, Jadhav S, Wadgoankar V, et al. Airway management and bronchoscopic treatment of subglottic and tracheal stenosis using holmium laser with balloon dilatation. *Indian J Otolaryngol Head Neck Surg* 2019;71:453–458.
- Shadmehr MB, Abbasidezfouli A, Farzanegan R, et al. The role of systemic steroids in postintubation tracheal stenosis: a randomized clinical trial. *Ann Thorac Surg* 2017;103:246–253.
- Choi JS, Kim JM, Kim JW, Kim YM, Park IS, Yang SG. Prevention of tracheal inflammation and fibrosis using nitinol stent coated with doxycycline. *Laryngoscope* 2018;128:1558–1563.
- Olmos-Zuniga JR, Silva-Martinez M, Jasso-Victoria R, et al. Effects of pirfenidone and collagen-polyvinylpyrrolidone on macroscopic and microscopic changes, TGF-beta1 expression, and collagen deposition in an experimental model of tracheal wound healing. *Biomed Res Int* 2017;2017:6471071.
- Motz KM, Yin LX, Samad I, et al. Quantification of inflammatory markers in laryngotracheal stenosis. *Otolaryngol Head Neck Surg* 2017;157:466–472.
- Hillel AT, Ding D, Samad I, Murphy MK, Motz K. T-helper 2 lymphocyte immunophenotype is associated with iatrogenic laryngotracheal stenosis. *Laryngoscope* 2019;129:177–186.
- Hillel AT, Samad I, Ma G, et al. Dysregulated macrophages are present in bleomycin-induced murine laryngotracheal stenosis. *Otolaryngol Head Neck Surg* 2015;153:244–250.
- Davis RJ, Lina I, Ding D, et al. Increased expression of PD-1 and PD-L1 in patients with laryngotracheal stenosis. *Laryngoscope* 2020;131:967–974.
- Hu HH, Wu FJ, Zhang JS, Chen E. Treatment of secondary benign airway stenosis after tracheotomy with Montgomery T-tube. *Math Biosci Eng* 2019;16:7839–7849.
- Smith ME, Elstad M. Mitomycin C and the endoscopic treatment of laryngotracheal stenosis: are two applications better than one? *Laryngoscope* 2009;119:272–283.
- Murgu SD, Colt HG, Mukai D, Brenner M. Multimodal imaging guidance for laser ablation in tracheal stenosis. *Laryngoscope* 2010;120:1840–1846.
- Syed F, Ahmadi E, Iqbal SA, Singh S, McGrouther DA, Bayat A. Fibroblasts from the growing margin of keloid scars produce higher levels of collagen I and III compared with intralesional and extralesional sites: clinical implications for lesional site-directed therapy. *Br J Dermatol* 2011;164:83–96.
- Hillel AT, Namba D, Ding D, Pandian V, Elisseeff JH, Horton MR. An in situ, in vivo murine model for the study of laryngotracheal stenosis. *JAMA Otolaryngol Head Neck Surg* 2014;140:961–966.
- Wu P, Tang Y, Fang X, et al. Metformin suppresses hypopharyngeal cancer growth by epigenetically silencing long non-coding RNA SNHG7 in FaDu cells. *Front Pharmacol* 2019;10:143.
- Pratsinisi H, Giannouli CC, Zervolea I, Psarras S, Stathakos D, Kletsas D. Differential proliferative response of fetal and adult human skin fibroblasts to transforming growth factor-beta. *Wound Repair Regen* 2004;12:374–383.
- Massague J. TGFbeta signalling in context. *Nat Rev Mol Cell Biol* 2012;13:616–630.
- Leask A, Abraham DJ. TGF-beta signaling and the fibrotic response. *FASEB J* 2004;18:816–827.
- van der Veer WM, Bloemen MC, Ulrich MM, et al. Potential cellular and molecular causes of hypertrophic scar formation. *Burns* 2009;35:15–29.
- Ghosh A, Malaisrie N, Leahy KP, et al. Cellular adaptive inflammation mediates airway granulation in a murine model of subglottic stenosis. *Otolaryngol Head Neck Surg* 2011;144:927–933.
- Richeldi L, du Bois RM, Raghu G, et al. Efficacy and safety of nintedanib in idiopathic pulmonary fibrosis. *N Engl J Med* 2014;370:2071–2082.
- Akhurst RJ, Hata A. Targeting the TGFbeta signalling pathway in disease. *Nat Rev Drug Discov* 2012;11:790–811.
- Deryck R, Zhang YE. Smad-dependent and Smad-independent pathways in TGF-beta family signalling. *Nature* 2003;425:577–584.
- Ying HZ, Chen Q, Zhang WY, et al. PDGF signalling pathway in hepatic fibrosis pathogenesis and therapeutics (review). *Mol Med Rep* 2017;16:7879–7889.
- Brewer JR, Mazot P, Soriano P. Genetic insights into the mechanisms of Fgf signalling. *Genes Dev* 2016;30:751–771.
- Lin X, Wen J, Liu R, Gao W, Qu B, Yu M. Nintedanib inhibits TGF-beta-induced myofibroblast transdifferentiation in human Tenon's fibroblasts. *Mol Vis* 2018;24:789–800.
- Overed-Sayer C, Miranda E, Dunmore R, et al. Inhibition of mast cells: a novel mechanism by which nintedanib may elicit anti-fibrotic effects. *Thorax* 2020;75:754–763.